

The effect of carbon nanotubes agglomeration on vibrational response of thick functionally graded sandwich plates

Vahid Tahouneh*

Young Researchers and Elite Club, Islamshahr Branch, Islamic Azad University, Islamshahr, Iran

(Received January 25, 2017, Revised May 21, 2017, Accepted June 02, 2017)

Abstract. In the present work, by considering the agglomeration effect of single-walled carbon nanotubes, free vibration characteristics of functionally graded (FG) nanocomposite sandwich plates resting on Pasternak foundation are presented. The volume fractions of randomly oriented agglomerated single-walled carbon nanotubes (SWCNTs) are assumed to be graded in the thickness direction. To determine the effect of CNT agglomeration on the elastic properties of CNT-reinforced composites, a two-parameter micromechanical model of agglomeration is employed. In this research work, an equivalent continuum model based on the Eshelby-Mori-Tanaka approach is employed to estimate the effective constitutive law of the elastic isotropic medium (matrix) with oriented straight CNTs. The 2-D generalized differential quadrature method (GDQM) as an efficient and accurate numerical tool is used to discretize the equations of motion and to implement the various boundary conditions. The proposed rectangular plates have two opposite edges simply supported, while all possible combinations of free, simply supported and clamped boundary conditions are applied to the other two edges. The benefit of using the considered power-law distribution is to illustrate and present useful results arising from symmetric and asymmetric profiles. The effects of two-parameter elastic foundation modulus, geometrical and material parameters together with the boundary conditions on the frequency parameters of the laminated FG nanocomposite plates are investigated. It is shown that the natural frequencies of structure are seriously affected by the influence of CNTs agglomeration. This study serves as a benchmark for assessing the validity of numerical methods or two-dimensional theories used to analysis of laminated plates.

Keywords: Mori-Tanaka approach; two-parameter micromechanical model of agglomeration; sandwich structures; 2D generalized differential quadrature method; vibration analysis

1. Introduction

Nowadays, the use of carbon nanotubes in polymer/carbon nanotube composites has attracted wide attention (Wagner *et al.* 1997). A high aspect ratio, low weight of CNTs and their extraordinary mechanical properties (strength and flexibility) provide the ultimate reinforcement for the next generation of extremely lightweight but highly elastic and very strong advanced composite materials. On the other hand, by using of the polymer/CNT composites in advanced multilayered composite materials (sandwich structures) we can achieve structures with low weight, high strength and high stiffness in many structures of civil, mechanical and space engineering.

Functionally graded materials (FGMs) are advanced composite materials that are engineered to have a smooth spatial variation of material properties. This is achieved by fabricating the composite material to have a gradual spatial variation of the constituent materials' relative volume fractions and microstructure (Koizumi 1993). Plates fabricated from FGMs have several engineering applications. Malekzadeh *et al.* (2011) analyzed the free vibration

analysis of FGM thin-to-moderately thick annular plates subjected to thermal environment and supported on two-parameter elastic foundation using first order shear deformation theory (FSDT) as well as DQM. Chakraverty *et al.* (2007) presented the effect of nonhomogeneity of the material properties on the vibration frequencies of circular and elliptic plates. They used boundary characteristic orthogonal polynomials as the basis function in the Rayleigh Ritz method to solve the problem. Free vibration frequencies and modes of variable thickness thick annular isotropic and FGM plates were studied by Efraim and Eisenberger (2007) using exact element method. Hosseini-Hashemi *et al.* (2010) performed the vibration of piezoelectric coupled thick annular functionally graded plates (FGPs) subjected to different combinations of boundary conditions at the inner and outer edges of the annular plate on the basis of the Reddy's third-order shear deformation theory (TSDT). Free and forced vibration of FGM annular sectorial plates with simply supported radial edges and arbitrary circular edges were investigated by Nie and Zhong (2008). The inhomogeneity of the plate was characterized by taking exponential variation of Young's modulus and mass density of the material along the radial direction whereas Poisson's ratio was assumed to remain constant. Yas and Tahouneh (2012) investigated the free vibration analysis of thick FG annular plates on elastic foundations via differential quadrature method based on the

*Corresponding author, Ph.D.,
E-mail: vahid.th1982@gmail.com;
vahid.tahouneh@ut.ac.ir

three-dimensional elasticity theory. The same authors (Tahouneh and Yas 2012, 2013, Tahouneh 2014a, b) investigated the free vibration analysis of thick one- and two-directional FG annular sector plates on Pasternak elastic foundations using DQM. Tahouneh *et al.* (2013) studied free vibration characteristics of annular continuous grading fiber reinforced (CGFR) plates resting on elastic foundations using DQM. Arefi (2015) proposed an elastic solution for a curved beam made of functionally graded materials with different cross sections. The beam was loaded under pure bending. Using the linear theory of elasticity, the general relation for radial distribution of radial and circumferential stresses of arbitrary cross section was derived. Bennai *et al.* (2015) developed a new refined hyperbolic shear and normal deformation beam theory to study the free vibration and buckling of functionally graded (FG) sandwich beams under various boundary conditions. The effects of transverse shear strains as well as the transverse normal strain were taken into account. Tahouneh (2016) used a semi-analytical approach composed of differential quadrature method (DQM) and series solution to present a 3-D elasticity solution for free vibration analysis of thick continuously graded carbon nanotube-reinforced (CGCNR) rectangular plates; In this study, an equivalent continuum model based on the Eshelby-Mori-Tanaka approach was employed to estimate the effective constitutive law of the elastic isotropic medium (matrix) with oriented, straight carbon nanotubes (CNTs). Yas and Sobhani Aragh (2010) achieved the natural frequencies of rectangular continuous grading fiber reinforced (CGFR) plates resting on elastic foundations; The CGFR plate was simply supported at the edges and was assumed to have an arbitrary variation of fiber volume fraction in the thickness direction. The results obtained indicated the advantages of using CGFR plate with graded fiber volume fractions over traditional discretely laminated plates. Matsunaga (2008) analyzed the natural frequencies and buckling stresses of FG plates using a higher order shear deformation theory which are based on the through the thickness series expansion of the displacement components. Zhou *et al.* (2004) used Ritz method to analyze the free-vibration characteristics of rectangular thick plates resting on elastic foundations. Matsunaga (2000) investigated a two-dimensional, higher-order theory for analyzing the thick simply supported rectangular plates resting on elastic foundations. Hosseini-Hashemi *et al.* (2010) employed the differential quadrature method to investigate free vibration of FGM circular and annular sectorial thin plates of variable thickness, resting on the Pasternak elastic foundation.

The discovery of carbon nanotubes (CNTs) by Iijima (1991) has generated a great and sustained interest in carbon based materials and nanotechnologies. CNTs have been shown to possess exceptional electrical, mechanical and thermal properties, which are attractive for diverse potential applications ranging from nano-electronics to biomedical devices. A detailed summary of the mechanical properties of CNTs can be found in (Salvetat and Rubio 2002). The exceptional mechanical properties of CNTs have shown great promise for a wide variety of applications, such

as nanotransistors, nanofillers, semiconductors, hydrogen storage devices, structural materials, molecular sensors, field-emission-based displays, and fuel cells, to name just a few (Endo *et al.* 2004). The addition of nano-sized fibers or nanofillers, such as CNTs, can further increase the merits of polymer composites (Wernik and Meguid 2011). These nanocomposites, easily processed due to the small diameter of the CNTs, exhibit unique properties (Thostenson *et al.* 2001, Moniruzzaman and Winey 2006), such as enhanced modulus and tensile strength, high thermal stability and good environmental resistance. This behavior, combined with their low density makes them suitable for a broad range of technological sectors such as telecommunications, electronics (Valter *et al.* 2002) and transport industries, especially for aeronautic and aerospace applications where the reduction of weight is crucial in order to reduce the fuel consumption. For example, Qian *et al.* (2000) showed that the addition of 1wt.% (i.e., 1% by weight) multiwall CNT to polystyrene resulted in 36-42% and 25% increases in the elastic modulus and the break stress of the nanocomposite properties, respectively. In addition, Yokozeki *et al.* (2007) reported the retardation of the onset of matrix cracking in the composite laminates containing the cup-stacked CNTs compared to those without the cup-stacked CNTs. The properties of the CNT-reinforced composites (CNTRCs) depend on a variety of parameters including CNT geometry and the interphase between the matrix and CNT. Interfacial bonding in the inter-phase region between embedded CNT and its surrounding polymer is a crucial issue for the load transferring and reinforcement phenomena (Shokrieh and Rafiee 2010a). The traditional approach to fabricating nanocomposites implies that the nanotube is distributed either uniformly or randomly such that the resulting mechanical, thermal, or physical properties do not vary spatially at the macroscopic level. Experimental and numerical studies concerning CNTRCs have shown that distributing CNTs uniformly as the reinforcements in the matrix can achieve moderate improvement of the mechanical properties only (Qian *et al.* 2000, Seidel and Lagoudas 2006). This is mainly due to the weak interface between the CNTs and the matrix where a significant material property mismatch exists. The concept of FGM can be utilized for the management of a material's microstructure so that the vibrational behavior of a plate/shell structure reinforced by CNTs can be improved. According to a comprehensive survey of literature, the authors found that there are few research studies on the mechanical behavior of functionally graded CNTRC structures. For the first time, Shen (2009) suggested that the nonlinear bending behavior can be considerably improved through the use of a functionally graded distribution of CNTs in the matrix. He introduced the CNT efficiency parameter to account load transfer between the nanotube and polymeric phases. Compressive postbuckling and thermal buckling behavior of functionally graded nanocomposite plates reinforced by aligned, straight SWCNTs subjected to in-plane temperature variation were reported by Shen and Zhu (2010) and Shen and Zhang (2010). They found that in some cases the CNTRC plate with intermediate CNT volume fraction does not have

intermediate buckling temperature and initial thermal post buckling strength. Moreover, Ke *et al.* (2010) investigated the nonlinear free vibration of functionally graded CNTRC Timoshenko beams. They found that both linear and nonlinear frequencies of functionally graded CNTRC beam with symmetrical distribution of CNTs are higher than those of beams with uniform or unsymmetrical distribution of CNTs. Kamarian *et al.* (2015) studied vibration analysis of sandwich beams. The material properties of the FG nanocomposite sandwich beam are estimated using the Eshelby-Mori-Tanaka approach. Marin and Lupu (1998) obtained a spatial estimate, similar to that of Saint-Venant type by using a measure of Toupin type associated with the corresponding steady-state vibration and assuming that the exciting frequency was lower to a certain critical frequency. Marin (2010) extended the concept of domain of influence in order to cover the elasticity of microstretch materials. Sharma and Marin (2013) studied wave propagation in micropolar thermoelastic solid half space with distinct conductive and thermodynamic temperatures. Reflection of plane waves incident obliquely at the free surface of micropolar generalized thermoelastic solid half space with two temperature was investigated.

Though there are research works reported on general sandwich structures, very little work has been done to consider even the vibration behavior of FG sandwich structures (Anderson 2003, Kashtalyan and Menshkyova 2009). Li *et al.* (2008) studied free vibrations of FGSW rectangular plates with simply supported and clamped edges. Zenkour (2005a, b) presented a two-dimensional solution to study the bending, buckling and free vibration of simply supported FG ceramic-metal sandwich plates. Kamarian *et al.* (2013) studied free vibration of FGSW rectangular plates with simply supported edges and rested on elastic foundations using differential quadratic method. Very recently, Wang and Shen (2011) investigated the large amplitude vibration and the nonlinear bending of a sandwich plate with CNTRC face sheets resting on an elastic foundation on the basis of a micromechanical model and multi-scale approach. Tahouneh and Naei (2016) investigated free vibration and vibrational displacements of thick laminated curved panels with finite via DQ method. The material properties varied continuously through the layers' thickness according to a three-parameter power-law distribution. It was assumed that the inner surfaces of the functionally graded sheets are metal rich, while the outer surfaces of the layers could be metal rich, ceramic rich or made of a mixture of two constituents. Bouchafa *et al.* (2015) investigated thermal stresses and deflections of functionally graded sandwich plates via a new refined hyperbolic shear deformation theory. The sandwich plate faces were assumed to have isotropic, two-constituent material distribution through the thickness, and the modulus of elasticity, Poisson's ratio of the faces, and thermal expansion coefficients were assumed to vary according to a power law distribution in terms of the volume fractions of the constituents.

In all studies mentioned above, the material properties of functionally graded CNTRCs were assumed to be graded in the thickness direction, and were estimated through the

extended rule of mixture in which the CNT efficiency parameter was determined by matching the elastic modulus of CNTRCs observed from the MD simulation results with the numerical results obtained from the extended rule of mixture. On the other hand, the extended rule of mixture is not applicable when CNTs are oriented randomly in the matrix. CNTs have low bending stiffness (due to small diameter and small elastic modulus in the radial direction) and high aspect ratio, which make CNTs easy to agglomerate in a polymer matrix (Shaffer and Windle 1999, Vigolo *et al.* 2000). In order to achieve the desired properties of CNTRCs, it is critical to make CNTs uniformly dispersed in the matrix (Shi *et al.* 2004). It has been observed in CNTRCs that a large amount of the nanotubes are concentrated in agglomerates (Wuite and Adali 2005). Stephan *et al.* (2000) observed that in the 7.5 percent concentration sample, a large amount of CNTs are concentrated in aggregates. In some research works, Authors have considered agglomeration effect of single-walled carbon nanotubes in different types of structures (Kamarian *et al.* 2016, 2015, Heshmati and Yas 2013, Tornabene *et al.* 2016, Moradi-Dastjerdi *et al.* 2013).

The specific objective of the present investigation is to provide a 3-D elasticity solution for the analysis of the natural frequencies of functionally graded (FG) nanocomposite sandwich plates resting on Pasternak foundation. The volume fractions of randomly oriented agglomerated SWCNTs are assumed to be graded in the thickness direction of sheets. The direct application of CNTs properties in micromechanics models for predicting material properties of the nanotube/polymer composite is inappropriate without taking into account the effects associated with the significant size difference between a nanotube and a typical carbon fiber (Odegard *et al.* 2003). In other words, continuum micromechanics equations cannot capture the scale difference between the nano and micro levels. In order to overcome this limitation, a virtual equivalent fiber consisting of nanotube and its interphase which is perfectly bonded to surrounding resin is applied. A two-parameter micromechanics model of agglomeration is used to determine the effect of CNT agglomeration on the elastic properties of randomly oriented CNTRCs. In this research work, an equivalent continuum model based on the Eshelby-Mori-Tanaka approach is employed to estimate the effective constitutive law of the elastic isotropic medium (matrix) with oriented straight CNTs. In the present work, the generalized differential quadrature method (GDQM) approach is used to solve the governing equations of sandwich plates.

2. Material properties of CNTRCs

2.1 Properties of the equivalent fiber

In this section, a virtual equivalent fiber consisting of nanotube and its interphase, which is perfectly bonded to surrounding resin, is introduced to obtain the mechanical properties of the CNT/polymer composite by using the results of multiscale finite element method (FEM). The

equivalent fiber for SWCNT with chiral index of (10,10) is a solid cylinder with diameter of 1.424 nm. ROM is used inversely for calculating material properties of equivalent fiber (Tsai *et al.* 2003)

$$\begin{aligned} E_{LEF} &= \frac{E_{LC}}{V_{EF}} - \frac{E_M V_M}{V_{EF}} \\ \frac{1}{E_{TEF}} &= \frac{1}{E_{TC} V_{EF}} - \frac{V_M}{E_M V_{EF}} \\ \frac{1}{G_{EF}} &= \frac{1}{G_C V_{EF}} - \frac{V_M}{G_M V_{EF}} \\ \nu_{EF} &= \frac{\nu_C}{V_{EF}} - \frac{\nu_M V_M}{V_{EF}} \end{aligned} \quad (1)$$

where E_{LEF} , E_{TEF} , G_{EF} , ν_{EF} , E_{LC} , E_{TC} , G_C , ν_C , E_M , G_M , ν_M , V_{EF} , and V_M are respectively longitudinal modulus of equivalent fiber, transverse modulus of equivalent fiber, shear modulus of equivalent fiber, Poisson's ratio of equivalent fiber, longitudinal modulus of composites, transverse modulus of composites, shear modulus of composites, Poisson's ratio of composites, modulus of matrix, shear modulus of matrix, Poisson's ratio of matrix, volume fraction of the equivalent fiber, and volume fraction of the matrix. E_{LC} , G_C , and E_{TC} are obtained from multiscale FEM or molecular dynamics (MD) simulations, respectively. Mechanical properties of the developed equivalent fiber are listed in Table 1 (Shokrieh and Rafiee 2010b). It must be mentioned that in (Shokrieh and Rafiee 2010b), material properties of the matrix are as

$$E^m = 2.1 \text{ GPa}, \rho^m = 1150 \text{ kg/m}^3, \nu^m = 0.34$$

2.2 Effect of CNT agglomeration on the properties of the composite

It has been found that in CNTRCs due to large aspect ratio (usually >1000), low bending rigidity of CNTs and van der Waals forces, CNTs have a tendency to bundle or cluster together. The effect of nanotube agglomeration on the elastic properties of randomly oriented CNTRC is presented in this section. Shi *et al.* (2004) derived a two-parameter micromechanics model to determine the effect of nanotube agglomeration on the elastic properties of randomly oriented CNTRC (Fig. 1). It is assumed that a number of CNTs are UD throughout the matrix and that other CNTs appear in cluster form because of agglomeration, as shown in Fig. 1. The total volume of the CNTs in the representative

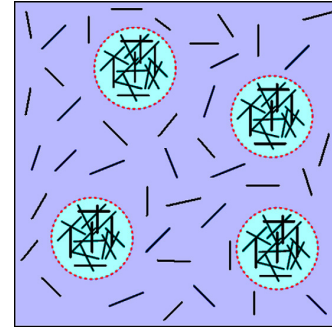


Fig. 1 Representative volume element (RVE) with Eshelby inclusion model of agglomeration of CNTs

volume element (RVE), denote by V_r , can be divided into the following two parts

$$V_r = V_r^{cluster} + V_r^m \quad (2)$$

where $V_r^{cluster}$ represents the volumes of CNTs inside a cluster, and V_r^m is the volume of CNTs in the matrix and outside the clusters. The two parameters used to describe the agglomeration are defined as

$$\mu = \frac{V_r^{cluster}}{V}, \eta = \frac{V_r^{cluster}}{V_r} \quad 0 \leq \eta, \mu \leq 1 \quad (3)$$

where V is the volume of RVE, $V_r^{cluster}$ is the volume of clusters in the RVE. μ is the volume fraction of clusters with respect to the total volume of the RVE and η is the volume ratio of the CNTs inside the clusters over the total CNT inside the RVE. $\mu = 1$ denotes the case that all CNTs are uniformly dispersed in the matrix and with the decrease of μ , the agglomeration degree of CNTs is more severe. If $\eta = 1$, all the nanotubes are located in the clusters. The case $\mu = \eta$ means that the volume fraction of CNTs inside the clusters is as same as that of CNTs outside the clusters (fully dispersed). When $\mu < \eta$, the bigger value of η denotes the more heterogeneous the spatial distribution of CNTs. Thus, we consider the CNTRC as a system consisting of clusters of sphere shape embedded in a matrix. We may first estimate, respectively, the effective elastic stiffness of the clusters and the matrix, and then calculate the overall property of the whole composite system. The effective bulk modulus K_{in} and shear modulus G_{in} of the cluster and the effective bulk modulus K_{out} and shear modulus G_{out} of the equivalent matrix outside the cluster can be calculated by (Shi *et al.* 2004)

$$K_{in} = K_m + \frac{f_r \eta (\delta_r - 3K_m \alpha_r)}{3(\mu - f_r \eta + f_r \eta \alpha_r)} \quad (4)$$

$$K_{out} = K_m + \frac{f_r (1-\eta) (\delta_r - 3K_m \alpha_r)}{3(1-\mu - f_r (1-\eta) + f_r (1-\eta) \alpha_r)} \quad (5)$$

$$G_{in} = G_m + \frac{f_r \eta (\eta_r - 2G_m \beta_r)}{2(\mu - f_r \eta + f_r \eta \alpha_r)} \quad (6)$$

$$G_{out} = G_m + \frac{f_r (1-\eta) (\eta_r - 2G_m \beta_r)}{2(1-\mu - f_r (1-\eta) + f_r (1-\eta) \alpha_r)} \quad (7)$$

Table 1 Material properties of equivalent fiber

Mechanical properties	Equivalent fiber (Tsai <i>et al.</i> 2003)
Longitudinal Young's modulus (Gpa)	649.12
Transverse Young's modulus (Gpa)	11.27
Longitudinal shear modulus (Gpa)	5.13
Poisson's ratio	0.284
Density (kg/m ³)	1400

where

$$\alpha_r = \frac{3(K_m + G_m) + k_r - l_r}{3(G_m + k_r)} \quad (8)$$

$$\beta_r = \frac{1}{5} \left[\frac{4G_m + 2k_r + l_r}{3(G_m + k_r)} + \frac{4G_m}{G_m + P_r} \right] + \frac{2}{5} \left[\frac{G_m(3K_m + G_m) + G_m(3K_m + 7G_m)}{G_m(3K_m + G_m) + m_r(3K_m + 7G_m)} \right] \quad (9)$$

$$\delta_r = \frac{1}{3} \left[\frac{(2k_r + l_r)(3K_m + 2G_m - l_r)}{G_m + k_r} + n_r + 2l_r \right] \quad (10)$$

$$\eta_r = \frac{1}{5} \left[\frac{2}{3}(n_r - l_r) + \frac{8G_m P_r}{G_m + P_r} + \frac{2(k_r - l_r)(2G_m + l_r)}{3(G_m + k_r)} \right] + \frac{1}{5} \left[\frac{8m_r G_m (3K_m + 4G_m)}{3K_m (m_r + G_m) + G_m (7m_r + G_m)} \right] \quad (11)$$

The subscripts m and r stand for the quantities of the matrix and the reinforcing phase, K_m and G_m are the bulk and shear moduli of the matrix, respectively, and k_r , l_r , m_r , n_r , and p_r are the Hill's elastic moduli for the reinforcing phase (CNTs), which can be found from the equality of two following matrices

$$C_r = \begin{bmatrix} n_r & l_r & l_r & 0 & 0 & 0 \\ l_r & k_r + m_r & k_r - m_r & 0 & 0 & 0 \\ l_r & k_r - m_r & k_r + m_r & 0 & 0 & 0 \\ 0 & 0 & 0 & p_r & 0 & 0 \\ 0 & 0 & 0 & 0 & m_r & 0 \\ 0 & 0 & 0 & 0 & 0 & p_r \end{bmatrix} \quad (12)$$

$$C_r = \begin{bmatrix} \frac{1}{E_L} & -\frac{\nu_{TL}}{E_T} & -\frac{\nu_{ZL}}{E_Z} & 0 & 0 & 0 \\ -\frac{\nu_{LT}}{E_L} & \frac{1}{E_T} & -\frac{\nu_{ZT}}{E_Z} & 0 & 0 & 0 \\ -\frac{\nu_{LZ}}{E_L} & -\frac{\nu_{TZ}}{E_T} & \frac{1}{E_Z} & 0 & 0 & 0 \\ 0 & 0 & 0 & \frac{1}{G_{TZ}} & 0 & 0 \\ 0 & 0 & 0 & 0 & \frac{1}{G_{ZL}} & 0 \\ 0 & 0 & 0 & 0 & 0 & \frac{1}{G_{LT}} \end{bmatrix}^{-1} \quad (13)$$

where E_L , E_T , E_Z , G_{TZ} , G_{ZL} , G_{LT} , ν_{LT} are material properties of the equivalent fiber, which can be determined from the inverse of the ROM. It must be noticed that before the use of the ROM, material properties of nanoscale RVE of nanocomposite must be obtained from multiscale FEM analysis or MD simulations. The effective bulk modulus K and the effective shear modulus G of the composite are derived from the MT method as follows (Shi *et al.* 2004)

$$K = K_{out} \left(1 + \frac{\mu \left(\frac{K_{in}}{K_{out}} - 1 \right)}{1 + \alpha(1 - \mu) \left(\frac{K_{in}}{K_{out}} - 1 \right)} \right) \quad (14)$$

$$G = G_{out} \left(1 + \frac{\mu \left(\frac{G_{in}}{G_{out}} - 1 \right)}{1 + \beta(1 - \mu) \left(\frac{G_{in}}{G_{out}} - 1 \right)} \right) \quad (15)$$

in which

$$\alpha = \frac{1 + S_{out}}{3(1 - S_{out})} \quad (16)$$

$$\beta = \frac{2(4 - 5S_{out})}{15(1 - S_{out})} \quad (17)$$

$$S_{out} = \frac{3K_{out} - 2G_{out}}{2(3K_{out} + G_{out})} \quad (18)$$

Finally, the effective Young's modulus E and Poisson's ratio ν of the composite are given by

$$E = \frac{9KG}{3K + G} \quad (19)$$

$$\nu = \frac{3K - 2G}{6K + 2G} \quad (20)$$

3. Problem description

Consider a sandwich rectangular plate with length a , width b , and thickness h as depicted in Fig. 2. The plate is supported by an elastic foundation with Winkler's (normal) and Pasternak's (shear) coefficients. The deformations defined with reference to a Cartesian coordinate system (x , y , z) are u , v and w in the x , y and z directions, respectively. In the present work, V_{cnt} and V_m are considered as the CNT and matrix volume fraction, respectively. We assume that the CNTs volume fraction varies through the thickness of FG-CNTR plate according to a generalized power-law distribution with four parameters as the following (Tornabene *et al.* 2015, Tornabene and Viola 2009)

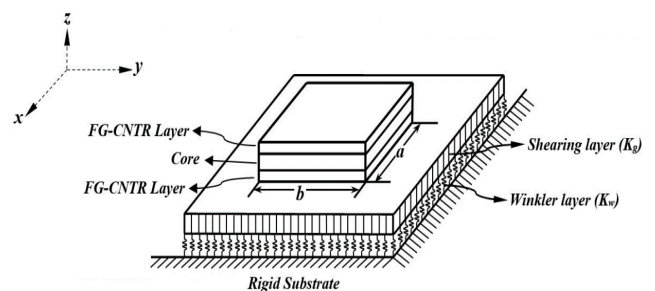


Fig. 2 Geometry of a FG-CNTR sandwich plate resting on an elastic foundation (the origin is placed in the middle of sandwich plate)

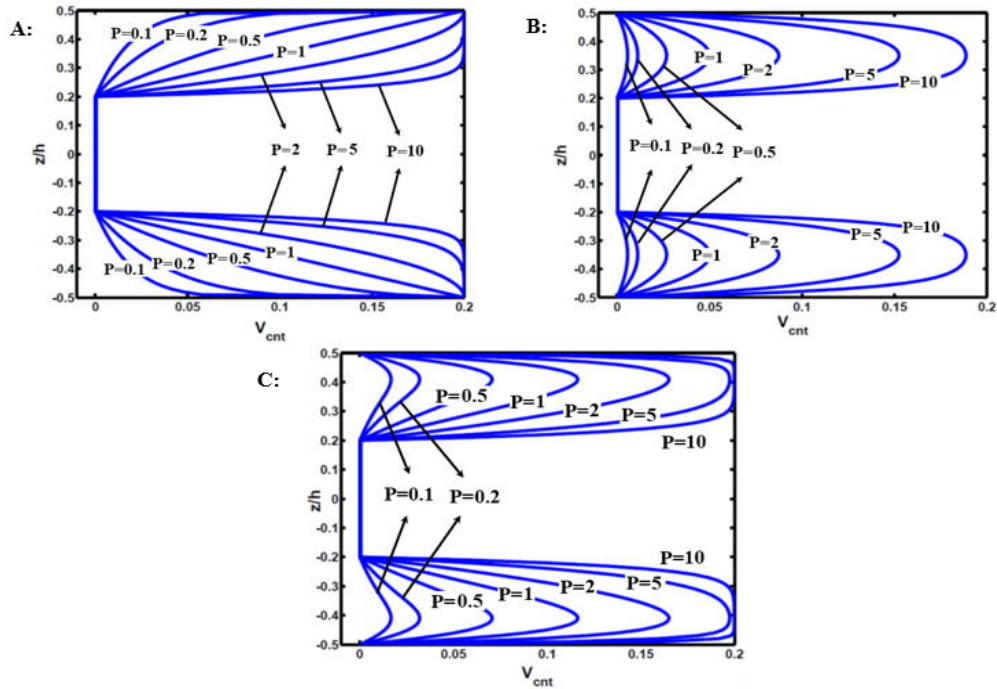


Fig. 3 Variation of the fiber volume fraction (V_{cnt}) through the thickness of the FG graded sandwich plate
 A: $a = 1, b = 0, c = 2$; B: $a = 1, b = 1, c = 2$; C: $a = 1, b = 1, c = 6$

$$V_{cnt} = \begin{cases} V^* \left(1 - \left(1 - a \left(1 - \frac{z+0.5}{h_f} \right) + b \left(1 - \frac{z+0.5}{h_f} \right)^c \right)^p \right), & -0.5h \leq z \leq -0.5h + h_f \\ 0, & -0.5h + h_f \leq z \leq 0.5h - h_f \\ V^* \left(1 - \left(1 - a \left(1 + \frac{z-0.5}{h_f} \right) + b \left(1 + \frac{z-0.5}{h_f} \right)^c \right)^p \right), & 0.5h - h_f \leq z \leq 0.5h \end{cases} \quad (21)$$

where h and h_f are the thicknesses of plate and the face sheets, respectively, V^* is the maximum possible amount of CNT volume fraction in the face sheets. Furthermore, volume fraction index p ($0 \leq p \leq \infty$) and the parameters a , b , and c indicate the CNT volume fraction profile through the thickness of structure. It should be noticed that the values of parameters a , b , and c must be chosen so that ($0 \leq V_{cnt} \leq V^*$). According to relation Eq. (21), the core of structure does not contain CNT, whereas the lower and upper face sheets are made of a mixture of the two constituents. Various material profiles through the thickness of face sheets can be illustrated by using the four-parameter power-law distribution. The through-thickness variations of volume fraction for some profiles are illustrated in Fig. 3 for different amounts of parameter b , c and p .

4. Governing equations and solution procedure

The mechanical constitutive relations that relate the stresses to the strains are as follows

$$\sigma_{ij} = \lambda \varepsilon_{kk} \delta_{ij} + 2\psi \varepsilon_{ij} \quad (22)$$

where λ and ψ are the Lamé constants, ε_{ij} is the infinitesimal strain tensor and δ_{ij} is the Kronecker delta. In the absence of body forces, the equations of motion are as follows

$$\begin{aligned} \frac{\partial \sigma_x}{\partial x} + \frac{\partial \tau_{xy}}{\partial y} + \frac{\partial \tau_{xz}}{\partial z} &= \rho \frac{\partial^2 u}{\partial t^2}, \\ \frac{\partial \tau_{xy}}{\partial x} + \frac{\partial \sigma_y}{\partial y} + \frac{\partial \tau_{yz}}{\partial z} &= \rho \frac{\partial^2 v}{\partial t^2}, \\ \frac{\partial \tau_{xz}}{\partial x} + \frac{\partial \tau_{yz}}{\partial y} + \frac{\partial \sigma_z}{\partial z} &= \rho \frac{\partial^2 w}{\partial t^2} \end{aligned} \quad (23)$$

The infinitesimal strain tensor is related to the displacements as follows

$$\begin{aligned} \varepsilon_x &= \frac{\partial u}{\partial x}, \varepsilon_y = \frac{\partial v}{\partial y}, \varepsilon_z = \frac{\partial w}{\partial z}, \gamma_{xy} = \frac{\partial u}{\partial y} + \frac{\partial v}{\partial x} \\ \gamma_{xz} &= \frac{\partial u}{\partial z} + \frac{\partial w}{\partial x}, \gamma_{yz} = \frac{\partial v}{\partial z} + \frac{\partial w}{\partial y} \end{aligned} \quad (24)$$

where u , v and w are displacement components along the x , y and z axes, respectively. Upon substitution Eq. (24) into Eq. (22) and then into Eq. (23), the equations of motion in terms of displacement components with infinitesimal deformations can be written as

$$\begin{bmatrix} F_{1x} & F_{1y} & F_{1z} \\ F_{2x} & F_{2y} & F_{2z} \\ F_{3x} & F_{3y} & F_{3z} \end{bmatrix} \begin{Bmatrix} u \\ v \\ w \end{Bmatrix} = \begin{Bmatrix} \rho \frac{\partial^2 u}{\partial t^2} \\ \rho \frac{\partial^2 v}{\partial t^2} \\ \rho \frac{\partial^2 w}{\partial t^2} \end{Bmatrix} \quad (25)$$

The related boundary conditions at $z = -h/2$ and $h/2$ are

as follows

$$\text{at } z = -h/2$$

$$\begin{aligned} \sigma_{zx} &= 0, \\ \sigma_{zy} &= 0, \sigma_{zz} = K_w w - K_g \left(\frac{\partial^2 w}{\partial x^2} + \frac{\partial^2 w}{\partial y^2} \right) \end{aligned} \quad (26)$$

$$\text{at } z = h/2$$

$$\sigma_{zx} = 0, \sigma_{zy} = 0, \sigma_{zz} = 0 \quad (27)$$

where σ_{ij} are the components of stress tensor; K_w and K_g are Winkler and shearing layer elastic coefficients of the foundation. The stress components are related to the displacement components using the three-dimensional constitutive relations as

$$\begin{aligned} \sigma_x &= c_{11} \frac{\partial u}{\partial x} + c_{12} \frac{\partial v}{\partial y} + c_{13} \frac{\partial w}{\partial z}, \sigma_{yz} = c_{44} \left(\frac{\partial w}{\partial y} + \frac{\partial v}{\partial z} \right) \\ \sigma_y &= c_{12} \frac{\partial u}{\partial x} + c_{22} \frac{\partial v}{\partial y} + c_{23} \frac{\partial w}{\partial z}, \sigma_{xz} = c_{55} \left(\frac{\partial u}{\partial z} + \frac{\partial w}{\partial x} \right) \\ \sigma_z &= c_{13} \frac{\partial u}{\partial x} + c_{23} \frac{\partial v}{\partial y} + c_{33} \frac{\partial w}{\partial z}, \sigma_{xy} = c_{66} \left(\frac{\partial v}{\partial x} + \frac{\partial u}{\partial y} \right) \end{aligned} \quad (28)$$

Different types of classical boundary conditions at the edges of the plate can be stated as

- Simply supported (S)

$$\sigma_{yy} = 0, w = 0, u = 0 \quad (29)$$

- Clamped (C)

$$u = 0, v = 0, w = 0 \quad (30)$$

- Free (F)

$$\sigma_{yy} = 0, \sigma_{xy} = 0, \sigma_{yz} = 0 \quad (31)$$

Here, plates with two opposite edges at $x = -a/2$ and $a/2$ simply supported and arbitrary conditions at edges $y = -b/2$ and $b/2$ are considered. For free vibration analysis, by adopting the following form for the displacement components the boundary conditions at edges $x = -a/2$ and $a/2$ are satisfied

$$\begin{aligned} u(x, y, z, t) &= U_m(y, z, t) \cos(m\pi(x + a/2)/a) e^{i\omega t} \\ v(x, y, z, t) &= V_m(y, z, t) \sin(m\pi(x + a/2)/a) e^{i\omega t} \\ w(x, y, z, t) &= W_m(y, z, t) \sin(m\pi(x + a/2)/a) e^{i\omega t} \end{aligned} \quad (32)$$

where m is the wave number along the x - direction, ω is the natural frequency and $i (= \sqrt{-1})$ is the imaginary number. Substituting for displacement components from Eq. (32) into the equations of motion which obtained in terms of displacement components, the coupled partial differential equations are reduced to a set of coupled ordinary differential equations (ODE). The geometrical and natural boundary can also be simplified, however, for brevity purpose, they are not shown here.

It is necessary to develop appropriate methods to investigate the mechanical responses of functionally graded (FG) nanocomposite sandwich plates. But, due to the complexity of the problem caused by the inhomogeneity, it is difficult to obtain the exact solution. In this paper, the generalized differential quadrature method (GDQM) approach is used to solve the governing equations of rectangular plates.

Substituting for displacement components from Eq. (32) into Eq. (25), and then using GDQ method to discretize the equations of motion, one can get the following equations (A brief review of GDQ method is given in Shu 2000, Shu and Richards 1992):

- In the x -direction

$$\begin{aligned} &-(c_{11})_{jk} \left(\frac{m\pi}{a} \right)^2 U_{mjk} + (c_{12})_{jk} \\ &\left(\frac{m\pi}{a} \right) \sum_{n=1}^{N_y} A_{jn}^y V_{mnk} + (c_{13})_{jk} \left(\frac{m\pi}{a} \right) \\ &\sum_{n=1}^{N_z} A_{kn}^z W_{mjn} + (c_{66})_{jk} \left(\frac{m\pi}{a} \sum_{n=1}^{N_y} A_{jn}^y V_{mnk} + \right. \\ &\left. \sum_{n=1}^{N_y} B_{jn}^y U_{mnk} \right) + \left(\frac{\partial c_{55}}{\partial z} \right)_{jk} \left(\frac{m\pi}{a} W_{mjk} + \right. \\ &\left. \sum_{n=1}^{N_z} A_{kn}^z U_{mjn} \right) + (c_{55})_{jk} \left(\frac{m\pi}{a} \sum_{n=1}^{N_z} A_{kn}^z W_{mjn} + \right. \\ &\left. \sum_{n=1}^{N_z} B_{kn}^z U_{mjn} \right) = -\rho_{jk} \omega^2 U_{mjk} \end{aligned} \quad (33)$$

- In the y -direction

$$\begin{aligned} &(c_{66})_{jk} \left(-\left(\frac{m\pi}{a} \right)^2 V_{mjk} + \left(\frac{-m\pi}{a} \right) \sum_{n=1}^{N_y} A_{jn}^y U_{mnk} \right) + \\ &(c_{12})_{jk} \left(\left(\frac{-m\pi}{a} \right) \sum_{n=1}^{N_y} A_{jn}^y U_{mnk} \right) \\ &+ (c_{22})_{jk} \sum_{n=1}^{N_y} B_{jn}^y V_{mnk} + (c_{23})_{jk} \left(\sum_{n=1}^{N_y} \sum_{r=1}^{N_z} A_{kr}^z A_{jn}^y W_{mnr} \right) + \\ &\left(\frac{\partial c_{44}}{\partial z} \right)_{jk} \left(\sum_{n=1}^{N_z} A_{kn}^z V_{mjn} + \sum_{n=1}^{N_y} A_{jn}^y W_{mnk} \right) + \\ &(c_{44})_{jk} \left(\sum_{n=1}^{N_z} B_{kn}^z V_{mjn} + \right. \\ &\left. \sum_{n=1}^{N_y} \sum_{r=1}^{N_z} A_{kr}^z A_{jn}^y W_{mnr} \right) = -\rho_{jk} \omega^2 V_{mjk} \end{aligned} \quad (34)$$

- In the z -direction

$$(c_{55})_{jk} \left(-\left(\frac{m\pi}{a} \right)^2 W_{mjk} - \frac{m\pi}{a} \sum_{n=1}^{N_z} A_{kn}^z U_{mjn} \right) + \quad (35)$$

$$\begin{aligned}
 & (c_{55})_{jk} \left(-\left(\frac{m\pi}{a}\right)^2 W_{mjk} - \frac{m\pi}{a} \sum_{n=1}^{N_z} A_{kn}^z U_{mjn} \right) + \\
 & (c_{44})_{jk} \left(\sum_{n=1}^{N_y} \sum_{r=1}^{N_z} A_{kr}^z A_{jn}^y V_{mnr} + \sum_{n=1}^{N_y} B_{jn}^y W_{mnk} \right) + \\
 & \left(\frac{\partial c_{13}}{\partial z} \right)_{jk} \left(-\frac{m\pi}{a} U_{mjk} \right) + (c_{13})_{jk} \left(-\frac{m\pi}{a} \sum_{n=1}^{N_z} A_{kn}^z U_{mjn} \right) \\
 & + \left(\frac{\partial c_{23}}{\partial z} \right)_{jk} \sum_{n=1}^{N_y} A_{jn}^y V_{mnk} + (c_{23})_{jk} \sum_{n=1}^{N_y} \sum_{r=1}^{N_z} A_{kr}^z A_{jn}^y V_{mnr} \\
 & + \left(\frac{\partial c_{33}}{\partial z} \right)_{jk} \sum_{n=1}^{N_z} A_{kn}^z W_{mjn} + (c_{33})_{jk} \sum_{n=1}^{N_z} B_{kn}^z W_{mjn} \\
 & = -\rho_{jk} \omega^2 W_{mjk}
 \end{aligned} \tag{35}$$

where A_{ij}^y, A_{ij}^z and B_{ij}^y, B_{ij}^z are the first and second order DQ weighting coefficients in the y - and z -directions, respectively. In a similar manner the boundary conditions can be discretized. In order to carry out the eigenvalue analysis, the domain and boundary nodal displacements should be separated. In vector forms, they are denoted as $\{d\}$ and $\{b\}$, respectively. Based on this definition, the discretized form of the equations of motion and the related boundary conditions can be represented in the matrix form as:

Equations of motion

$$\left[[K_{db}] [K_{dd}] \right] \begin{Bmatrix} \{b\} \\ \{d\} \end{Bmatrix} - \omega^2 [M] \{d\} = \{0\} \tag{36}$$

and boundary conditions

$$[K_{bd}] \{d\} + [K_{bb}] \{b\} = \{0\} \tag{37}$$

Eliminating the boundary degrees of freedom in Eq. (36) using Eq. (37), this equation becomes

$$[K] - \omega^2 [M] \{d\} = \{0\} \tag{38}$$

where $[K] = [K_{dd}] - [K_{db}][K_{bb}]^{-1}[K_{bd}]$. The above eigenvalue system of equations can be solved to find the natural frequencies and mode shapes of the plates.

5. Numerical results and discussion

Firstly, the results are compared with those of 1-D conventional functionally graded rectangular plates, and then, the results of the presented formulations are given in the form of convergence studies with respect to N_z and N_y , the number of discrete points distributed along the thickness and width of the plate, respectively. The boundary conditions of the plate are specified by the letter symbols, for example, S - C - S - F denotes a plate with edges $x = -a/2$ and $a/2$ simply supported (S), edge $y = -b/2$ clamped (C) and edge $y = b/2$ free (F). As a first example, the properties of the plate are assumed to vary through the thickness of the

plate with a desired variation of the volume fractions of the two materials in between the two surfaces. The modulus of elasticity E and mass density ρ are assumed to be in terms of a simple power law distribution and Poisson's ratio ν is assumed to be constant as follows

$$\begin{aligned}
 E(z) &= E_M + E_{CM} V_f, \nu(z) = \nu_0, \rho(z) = \rho_M + \rho_{CM} V_f \\
 E_{CM} &= E_C - E_M, \rho_{CM} = \rho_C - \rho_M, V_f = (0.5 + z/h)^p
 \end{aligned} \tag{39}$$

where $-h/2 \leq z \leq h/2$ and p is the power law index which takes values greater than or equal to zero. Subscripts M and C refer to the metal and ceramic constituents which denote the material properties of the bottom and top surface of the plate, respectively. The mechanical properties are as follows:

- Metal (Aluminum, Al)

$$E_M = 70 * 10^9 \text{ N/m}^2, \nu = 0.3, \rho_M = 2702 \text{ kg/m}^3$$

- Ceramic (Alumina, Al_2O_3)

$$E_C = 380 * 10^9 \text{ N/m}^2, \nu = 0.3, \rho_C = 3800 \text{ kg/m}^3$$

In Table 2, the first seven non-dimensional natural frequency parameters of simply supported thick FG plate are compared with those of Matsunaga (2008) and Yas and Sobhani (2010). As the second example, in order to validate the results for plates on an elastic foundation, the results for the first three natural frequency parameters of isotropic thick plate with two different values of thickness-to-length ratios and different values of Winkler elastic coefficient are presented in Table 3. They are compared with those of Zhou *et al.* (2004), Matsunaga (2000), and Yas and Sobhani (2010). In this example the non-dimensional natural frequency, Winkler and shearing layer elastic coefficients are as follows

$$\begin{aligned}
 \lambda &= \omega b^2 / \pi^2 \sqrt{\rho_C h / D_C}, D_C = E_C h^3 / 12(1 - \nu_C^2) \\
 k_g &= K_g b^2 / D_C, k_w = K_w b^4 / D_C
 \end{aligned} \tag{40}$$

According to the data presented in the above-mentioned tables, excellent solution agreements can be observed between the present method and those of the other methods. Based on the above studies, a numerical value of $N_z = N_y = 13$ is used for the next studies. The variation of CNT distribution through the plate is assumed as follows (Fig. 4)

$$V_{cnt} = \left\{ \begin{array}{l} 2 * \left(\frac{2|z|}{h}\right) * V_{CNT}^*, FG - X(\text{Type 1}) \\ V_{CNT}^*, UD(\text{Type 2}) \\ \left(1 + \frac{2z}{h}\right) * V_{CNT}^*, FG - \Lambda(\text{Type 3}) \\ 2 * \left(1 - \frac{2|z|}{h}\right) * V_{CNT}^*, FG - \diamond(\text{Type 4}) \end{array} \right\} \tag{41}$$

where V_{CNT}^* is the CNT volume fraction. It should be noted that for both UD and FG cases the values of mass fractions of CNTs are considered to be the same. After demonstrating

Table 2 Convergence behavior and accuracy of the first seven non-dimensional natural frequencies ($\varpi = \omega h \sqrt{\rho_c / E_c}$) of a simply supported FG plate against the number of DQ grid points ($b/h = 2$)

P	N_z	N_y	ϖ_1	ϖ_2	ϖ_3	ϖ_4	ϖ_5	ϖ_6	ϖ_7	
0	7	7	0.5569	0.9395	0.9735	1.3764	1.5072	1.6064	1.7384	
		9	0.5570	0.9396	0.9741	1.3771	1.5083	1.6071	1.7401	
		13	0.5570	0.9396	0.9740	1.3774	1.5088	1.6076	1.7407	
	9	7	0.5573	0.9398	0.9735	1.3771	1.5087	1.6074	1.7403	
		9	0.5572	0.9400	0.9742	1.3777	1.5090	1.6079	1.7406	
		13	0.5572	0.9400	0.9741	1.3778	1.5096	1.6086	1.7405	
	13	7	0.5571	0.9401	0.9735	1.3779	1.5094	1.6083	1.7411	
		9	0.5572	0.9400	0.9742	1.3777	1.5090	1.6078	1.7405	
		13	0.5572	0.9400	0.9742	1.3777	1.5090	1.6078	1.7406	
		Matsunaga 2008	0.5572	0.9400	0.9742	1.3777	1.5090	1.6078	1.7406	
			Yas and Sobhani Aragh 2010	0.557243	0.940041	-	-	1.508987	-	1.740602
	0.5	7	7	0.4829	0.8222	0.8700	1.2250	1.3332	1.4364	1.5401
9			0.4828	0.8229	0.8707	1.2258	1.3337	1.4367	1.5429	
13			0.4830	0.8224	0.8706	1.2254	1.3338	1.4370	1.5424	
9		7	0.4833	0.8225	0.8701	1.2251	1.3335	1.4365	1.5402	
		9	0.4835	0.8240	0.8708	1.2257	1.3340	1.4370	1.5431	
		13	0.4836	0.8233	0.8707	1.2258	1.3340	1.4369	1.5426	
13		7	0.4836	0.8227	0.8701	1.2251	1.3334	1.4366	1.5402	
		9	0.4835	0.8231	0.8708	1.2259	1.3338	1.4370	1.5431	
		13	0.4835	0.8233	0.8709	1.2259	1.3339	1.4370	1.5425	
		Matsunaga 2008	0.4835	0.8233	0.8709	1.2259	1.3339	1.4370	1.5425	
			Yas and Sobhani Aragh 2010	0.482849	0.822358	-	-	1.332605	-	1.541085
1		7	7	0.4367	0.7476	0.7997	1.1158	1.2154	1.3085	1.4059
	9		0.4374	0.7477	0.8001	1.1165	1.2159	1.3090	1.4075	
	13		0.4373	0.7478	0.8005	1.1163	1.2162	1.3088	1.4077	
	9	7	0.4368	0.7477	0.7998	1.1159	1.2157	1.3088	1.4068	
		9	0.4374	0.7477	0.8003	1.1165	1.2161	1.3090	1.4076	
		13	0.4374	0.7478	0.8006	1.1165	1.2162	1.3090	1.4078	
	13	7	0.4368	0.7477	0.7999	1.1159	1.2158	1.3088	1.4070	
		9	0.4375	0.7478	0.8003	1.1165	1.2162	1.3091	1.4076	
		13	0.4375	0.7478	0.8005	1.1165	1.2163	1.3091	1.4077	
		Matsunaga 2008	0.4375	0.7477	0.8005	1.1166	1.2163	1.3091	1.4078	
			Yas and Sobhani Aragh 2010	0.437396	0.747514	-	-	1.216035	-	1.407459
	4	7	7	0.3565	0.5988	0.6249	0.8724	0.9589	1.0000	1.1029
9			0.3577	0.5995	0.6355	0.8729	0.9589	1.0007	1.1038	
13			0.3577	0.5996	0.6349	0.8728	0.9589	1.0003	1.1030	
9		7	0.3569	0.5989	0.6250	0.8726	0.9589	1.0001	1.1032	
		9	0.3579	0.5997	0.6357	0.8731	0.9589	1.0008	1.1040	
		13	0.3578	0.5997	0.6351	0.8730	0.9589	1.0005	1.1032	
13		7	0.3571	0.5991	0.6252	0.8727	0.9589	1.0001	1.1033	
		9	0.3579	0.5997	0.6357	0.8731	0.9589	1.0008	1.1040	
		13	0.3579	0.5997	0.6352	0.8731	0.9589	1.0008	1.1040	
		Matsunaga 2008	0.3579	0.5997	0.6352	0.8731	0.9591	1.0008	1.1040	
			Yas and Sobhani Aragh 2010	0.357758	0.599494	-	-	0.958764	-	1.103674

Table 2 Continued

P	N_z	N_y	ϖ_1	ϖ_2	ϖ_3	ϖ_4	ϖ_5	ϖ_6	ϖ_7
		7	0.3306	0.5454	0.5657	0.7866	0.8588	0.9043	0.9838
	7	9	0.3311	0.5460	0.5662	0.7890	0.8588	0.9047	0.9841
		13	0.3310	0.5459	0.5661	0.7881	0.8588	0.9050	0.9846
		7	0.3308	0.5455	0.5659	0.7870	0.8588	0.9044	0.9840
	9	9	0.3313	0.5461	0.5664	0.7892	0.8588	0.9048	0.9842
10		13	0.3312	0.5460	0.5663	0.7883	0.8588	0.9051	0.9846
		7	0.3309	0.5455	0.5660	0.7871	0.8588	0.9045	0.9840
		9	0.3313	0.5461	0.5664	0.7892	0.8588	0.9049	0.9844
	13	13	0.3313	0.5461	0.5664	0.7884	0.8588	0.9051	0.9847
		Matsunaga 2008	0.3313	0.5460	0.5664	0.7885	0.8588	0.9050	0.9847
		Yas and Sobhani Aragh 2010	0.331146	0.545833	-	-	0.858445	-	0.984365

Table 3 Comparison of the first three non-dimensional natural frequency parameters of a simply supported square isotropic plate on the elastic foundation ($k_g = 10$)

K_w	N_z	N_y	$b/h = 2$			$b/h = 5$		
			λ_{11}	λ_{12}	λ_{13}	λ_{11}	λ_{12}	λ_{13}
		7	1.6453	2.6906	3.8259	2.2325	4.4045	7.2429
	7	9	1.6461	2.6855	3.8264	2.2332	4.4058	7.2434
		13	1.6460	2.6848	3.8264	2.2330	4.4052	7.2433
		7	1.6455	2.6905	3.8261	2.2329	4.4046	7.2431
	9	9	1.6462	2.6857	3.8267	2.2334	4.4060	7.2436
0		13	1.6461	2.6850	3.8266	2.2333	4.4055	7.2435
		7	1.6455	2.6907	3.8262	2.2330	4.4049	7.2432
		9	1.6462	2.6857	3.8267	2.2334	4.4060	7.2436
	13	13	1.6462	2.6851	3.8267	2.2334	4.4057	7.2436
		Zhou <i>et al.</i> 2004	1.6462	2.6851	3.8268	2.2334	4.4056	7.2436
		Matsunaga 2000	1.6462	2.6851	3.8268	2.2334	4.4056	7.2436
		Yas and Sobhani Aragh 2010	1.646182	2.685124	3.826819	2.233409	4.405606	7.243589
		7	1.6569	2.6870	3.8261	2.2532	4.415	7.2474
	7	9	1.6575	2.6875	3.8280	2.2537	4.415	7.2484
		13	1.6574	2.6875	3.8271	2.2536	4.415	7.2483
		7	1.6572	2.6872	3.8262	2.2534	4.415	7.2481
	9	9	1.6577	2.6878	3.8282	2.2539	4.415	7.2487
10		13	1.6576	2.6876	3.8273	2.2538	4.415	7.2485
		7	1.6573	2.6873	3.8264	2.2535	4.415	7.2482
		9	1.6577	2.6878	3.8282	2.2539	4.415	7.2487
	13	13	1.6577	2.6878	3.8275	2.2539	4.415	7.2487
		Zhou <i>et al.</i> 2004	1.6577	2.6879	3.8274	2.2539	4.415	7.2487
		Matsunaga 2000	1.6577	2.6879	3.8274	2.2539	4.415	7.2488
		Yas and Sobhani Aragh 2010	1.657742	2.687861	3.827391	2.253924	4.415035	7.248745

the convergence and accuracy of the method, parametric studies for 3-D vibration analysis of functionally graded (FG) nanocomposite sandwich plates resting on Pasternak foundation for various length to width ratio (a/b) and different combinations of free, simply supported and

clamped boundary conditions at the edges, are computed.

A comprehensive study is also carried out to investigate the effect of CNTs agglomeration on the vibrational response of sandwich structures.

Before analyzing the free vibration of functionally

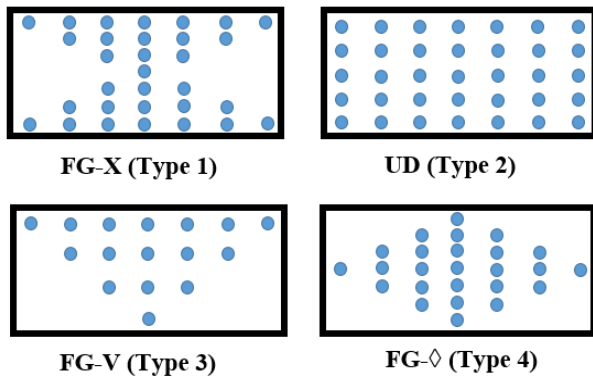


Fig. 4 Schematic configuration of a carbon nanotube-reinforced composite plate with four types of CNT distribution

graded (FG) nanocomposite sandwich plates, the effects of agglomeration degree (μ and η) on the effective longitudinal Young's modulus and Poisson's ratio of UD-CNTRC plate are investigated in Fig. 5. A represents the fact that the highest values of Young's modulus are attained for the agglomeration state of $\mu = \eta$ (fully dispersed), where the volume fraction of CNTs in the cluster and the matrix are equal. As it is observed, when μ is less than η ($\mu < \eta$), the effective Young's modulus increases with increasing the value of μ and has the maximum value when the CNTs are uniformly dispersed in the composite, i.e., $\mu = \eta$ and for $\mu > \eta$, the effective stiffness decreases with the increase of μ .

The effect of agglomeration degree on the Poisson's ratio for UD-plate is plotted in Fig. 5(b). In contrast to Young modulus behavior, with the increase of μ , Poisson's ratio decreases for $\mu < \eta$ and increases for $\mu > \eta$ due to the fact that the Poisson's ratio of the equivalent fiber described in properties of the equivalent fiber section is less than the Poisson's ratio of matrix.

Using the relations presented in material properties of CNTRCs and Problem description sections, it is also possible to observe the variations of the effective material properties through the thickness of the FGS-CNTR plate for different agglomeration parameters. For instance, by considering $h_1/h = 0.25$, $a = 1$, $b = 0$, $p = 1$, and $V^* = 30\%$, the variations of Young's modulus and Poisson's ratio of

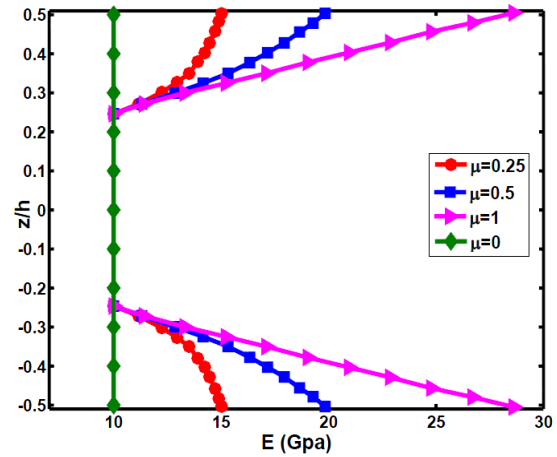


Fig. 6 The variation of Young's modulus along the thickness of the FGS-CNTR plate with agglomeration effect

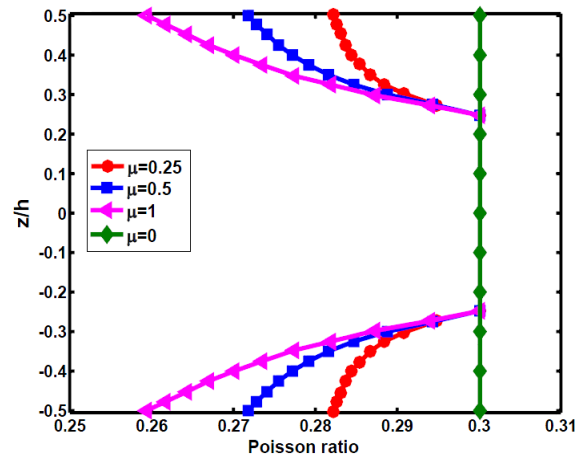


Fig. 7 The variation of Poisson's ratio along the thickness of the FGS-CNTR plate with agglomeration effect

FGS plates with respect to the different agglomeration parameters μ and $\eta = 1$ are illustrated in Figs. 6 and 7. As expected, at a constant value of z/h ratio, with the increase of parameter μ , the effective Young's modulus increases and on the other hand, the Poisson's ratio decreases, because $\mu < \eta = 1$. It is also completely obvious that the agglomeration

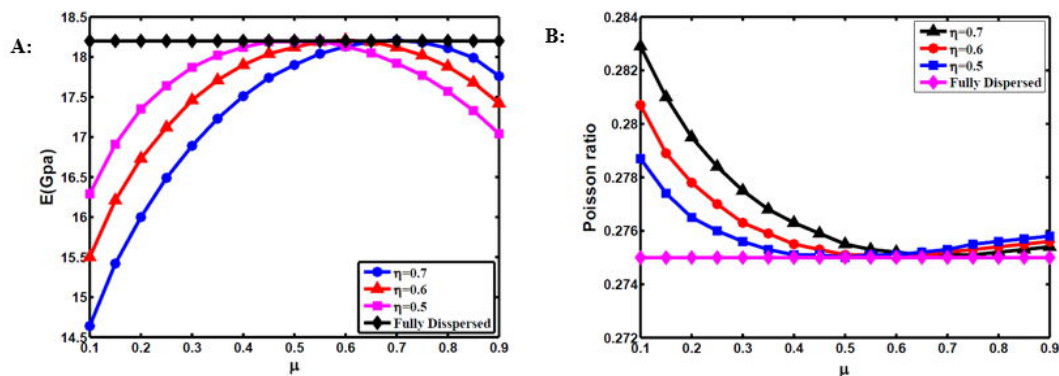


Fig. 5 Influence of CNT agglomeration parameters μ and η on the A: effective Young's modulus; B: Poisson's ratio of UD nanocomposite plate

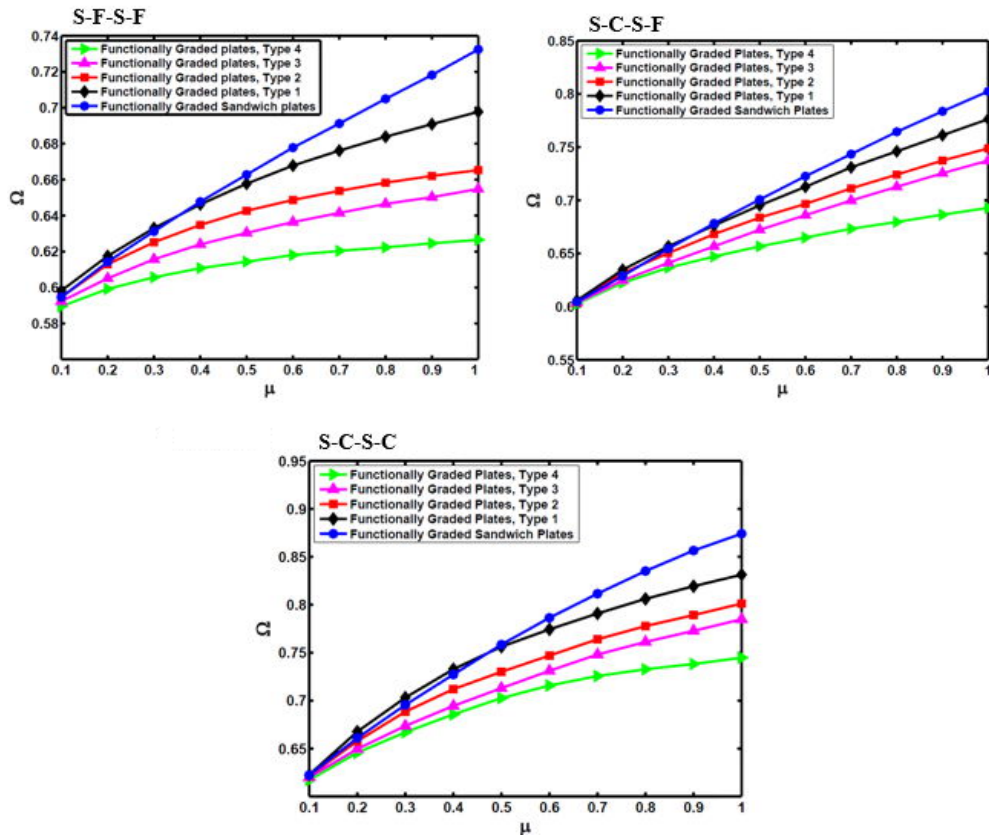


Fig. 8 The variation of frequency parameters versus agglomeration parameter for different types of CNTRC plates and boundary conditions ($\eta = 1, a/b = 1, b/h = 2, K_g = K_w = 10$)

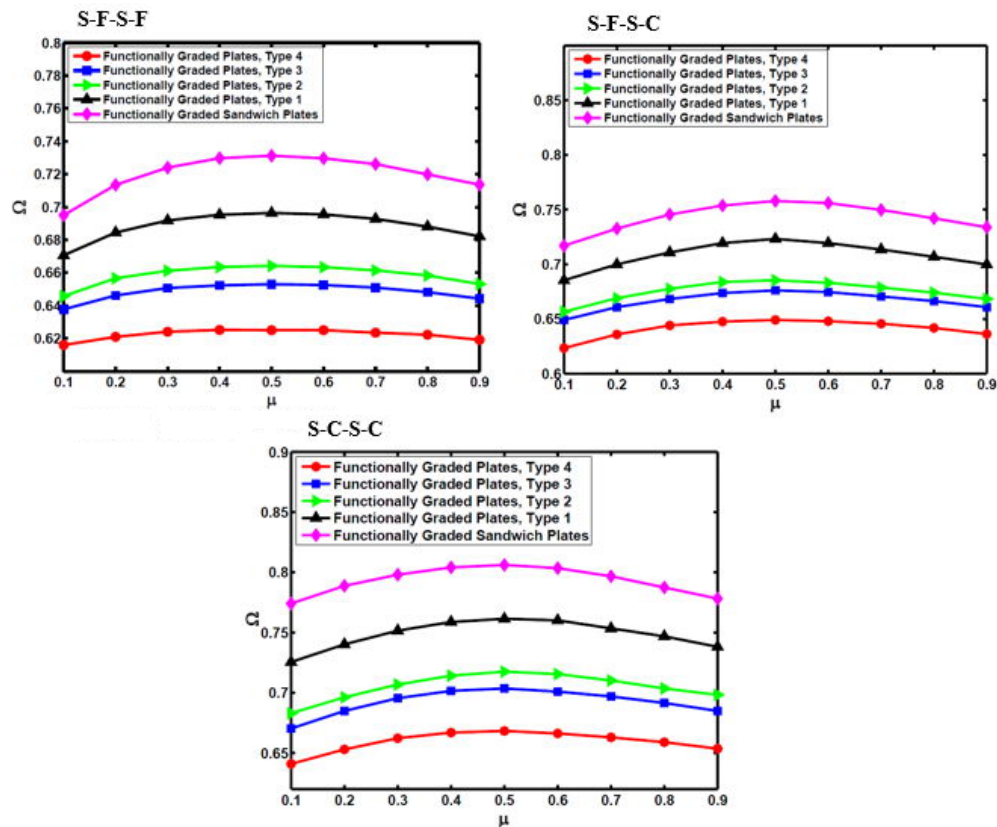


Fig. 9 The variation of frequency parameters versus agglomeration parameter for different types of CNTRC plates and boundary conditions ($\eta = 0.5, a/b = 1, b/h = 2$)

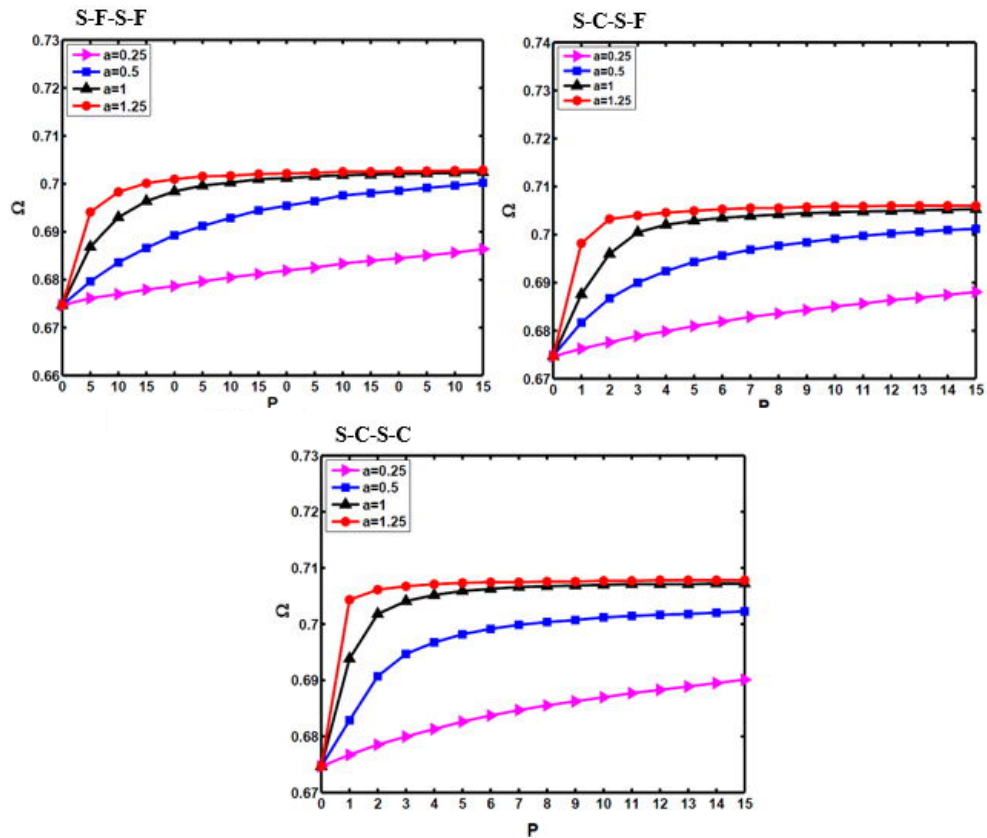


Fig. 10 Variation of the fundamental frequency parameter of CNTR plates for different type of boundary conditions versus the power-law exponent p ($a/b = 1$, $b/h = 2$, $K_g = K_w = 10$)

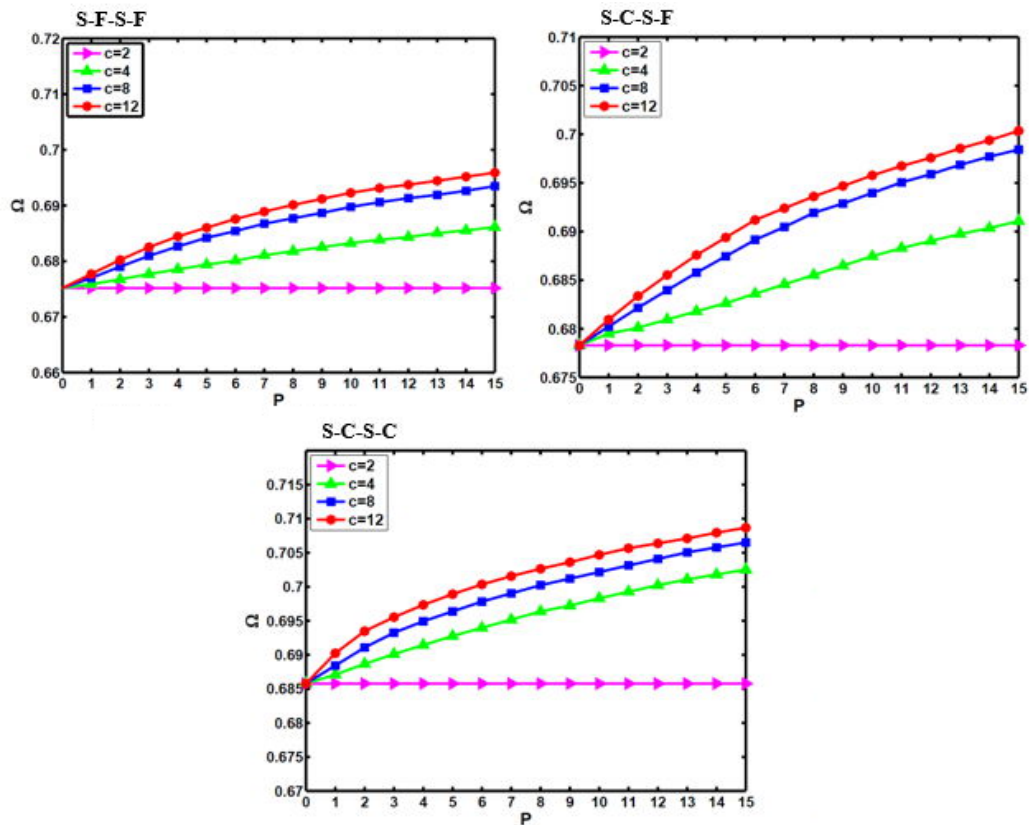


Fig. 11 Variation of the fundamental frequency parameter of FGS-CNTR plates for different types of boundary conditions versus the power-law exponent p ($a/b = 1$, $b/h = 2$, $K_g = K_w = 10$)

parameters have significant effects on the material properties. Therefore, it is concluded that CNTs agglomeration plays an important role in vibrational characteristics of FGS-CNTR plates.

Now free vibration characteristics of FGS-CNTR plates rested on Pasternak foundation is studied using MT approach based on the equivalent fiber discussed in Properties of the equivalent fiber section and using Table 1. Also, the material properties of the matrix are as

$$E^m = 2.1 \text{ Gpa}, \rho^m = 1150 \text{ kg/m}^3, \nu^m = 0.34$$

The non-dimensional natural frequency, Winkler and shearing layer elastic coefficients are as follows (Tahouneh and Naei 2014)

$$\Omega = \omega \frac{b^2}{\pi^2} \sqrt{\rho_m h / D_m}, D_m = E_m / 12(1 - \nu_m^2) \tag{42}$$

$$K_g = k_g b^2 / D_m, K_w = k_w b^4 / D_m$$

The effect of agglomeration on vibrational response of FG plates resting on a two-parameter elastic foundation for different boundary conditions are depicted in Fig. 8. It is clear the lowest magnitude frequency parameter is obtained by using a FG plates, Type 4 and followed by Type 3, 2, 1 and FG sandwich plate; respectively. It is also seen for great amount of η , for instance $\eta = 1$ and for small amount of μ , the FG sandwich plates have lower amount of frequency than FG Type 1. It should be noted that, for all the Types of CNTs distribution with the increase of μ , the frequency parameters increase. It can be seen that the discrepancies between frequencies for the plates with Type 3 and Type 2 material distribution of CNTs remain almost unaltered with the increase of μ .

Fig. 9 shows that for lower amount of η the frequency response of plates with different types of material distribution has changed. These figures reveal that with the increase of μ , the natural frequency increase but for μ approximately more than 0.5, the frequency parameters tend to decrease. The influence of the index p and parameters a on the fundamental frequency parameters of FGS-CNTR plate rested on Pasternak foundation is shown in Fig. 10 for S-F-S-F, S-F-S-C and S-C-S-C boundary conditions.

Fig. 10 shows the fundamental frequency parameters of the FGS-CNTR plate rested on Pasternak foundation versus the power-law index p for various values of the parameter a , when $b = 0.3$ and $c = 3$. In any cases, with the increase of parameter p the frequency parameter of sandwich plates increased. It should be taken into account that for small amount of a , the frequency parameter steadily increased but for great amount of this parameter the increase of frequency parameter happens sharply.

The influence of the parameter c on the free vibration of sandwich plates with FG-CNTR face sheets is investigated when parameter c varies from 2 to 12. As one can see from Fig. 11 with the increase of parameter c , the fundamental frequency increases. This is due to the fact that with the increase in the value of parameter c , the CNTs volume fraction and therefore the frequency parameters increase.

The effect of Winkler elastic coefficient on the non-

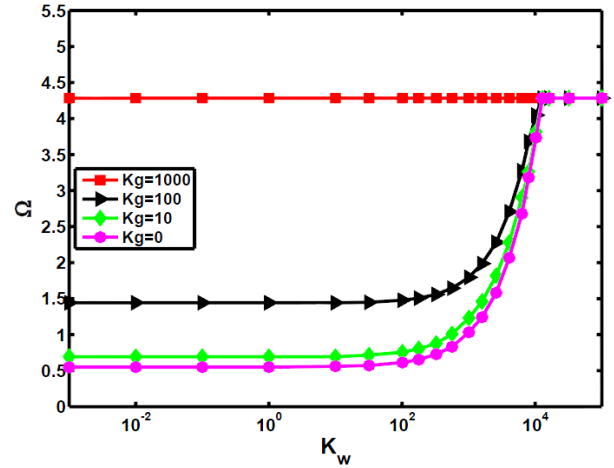


Fig. 12 Variation of the non-dimensional frequency parameter of S-F-S-F FG-CNTR plates versus Winkler elastic coefficient for different shearing layer elastic coefficients ($a/b = 1, b/h = 2, a = 1.25, p = 5, \eta = \mu = 0.5$)

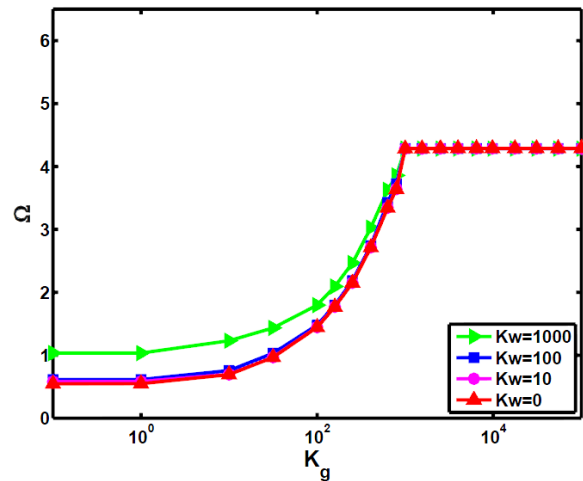


Fig. 13 Variation of frequency parameter versus shearing layer elastic coefficient for different values of Winkler elastic foundation stiffness for S-F-S-F FG-CNTR plates ($a/b = 1, b/h = 2, a = 1.25, p = 5, \eta = \mu = 0.5$)

dimensional natural frequency parameter at different values of shearing layer elastic coefficient is shown in Fig. 12. It is observed for the large values of Winkler elastic coefficient, the shearing layer elastic coefficient has less effect and the results become independent of it. In other word, the non-dimensional natural frequency parameters converge with increasing Winkler elastic coefficient of the foundation. It can be concluded from Fig. 12 that the non-dimensional natural frequency parameters converge at the large values of Winkler elastic coefficient. Fig. 13 shows the effect of shearing layer elastic coefficient on the non-dimensional natural frequency parameters for different values of Winkler elastic coefficient. It can be seen for the large values of shearing layer elastic coefficient, the Winkler elastic coefficient has less effect and the results become

independent of it. It results the variations of Winkler elastic coefficient has little effect on the non-dimensional frequency parameters at different values of shearing layer elastic coefficient.

6. Conclusions

In this research work, 2-D generalized differential quadrature method was employed to obtain a highly accurate semi-analytical solution for free vibration of functionally graded (FG) nanocomposite sandwich plates resting on Pasternak foundation under various boundary conditions. The study was carried out based on the three-dimensional, linear and small strain elasticity theory. The MT approach was implemented to estimate the effective material properties of the nanocomposite sandwich plate.

The agglomeration effect of single-walled carbon nanotubes, is considered in this study and it is shown that the natural frequencies of structure are seriously affected by the influence of CNTs agglomeration. Results presented the fact that mechanical properties and therefore free vibrations of FGS-CNTR plates are seriously affected by CNTs agglomeration. It was found that except some states, FGS types of structures improve the vibrational characteristics of CNTRCs. The effects of different boundary conditions, various geometrical parameters, different material profiles along the thickness and elastic coefficients of foundation of sandwich rectangular plates resting on a two-parameter elastic foundation were investigated.

References

- Anderson, T.A. (2003), "A 3-D elasticity solution for a sandwich composite with functionally graded core subjected to transverse loading by a rigid sphere", *Compos. Struct.*, **60**(3), 265-274.
- Arefi, M. (2015), "Elastic solution of a curved beam made of functionally graded materials with different cross sections", *Steel Compos. Struct., Int. J.*, **18**(3), 659-672.
- Bennai, R., Ait Atmane, H. and Tounsi, A. (2015), "A new higher-order shear and normal deformation theory for functionally graded sandwich beams", *Steel Compos. Struct., Int. J.*, **19**(3), 521-546.
- Bouchafa, A., Bouiadjra, M.B., Houari, M.S.A. and Tounsi, A. (2015), "Thermal stresses and deflections of functionally graded sandwich plates using a new refined hyperbolic shear deformation theory", *Steel Compos. Struct., Int. J.*, **18**(6), 1493-1515.
- Chakraverty, S., Jindal, R. and Agarwal, V.K. (2007), "Effect of nonhomogeneity on natural frequencies of vibration of elliptic plates", *Meccanica*, **42**(6), 585-599.
- Efraim, E. and Eisenberger, M. (2007), "Exact vibration analysis of variable thickness thick annular isotropic and FGM plates", *J. Sound Vib.*, **299**(4-5), 720-738.
- Endo, M., Hayashi, T., Kim, Y.A., Terrones, M. and Dresselhaus, M.S. (2004), "Applications of carbon nanotubes in the twenty-first century", *Phil. Trans. R. Soc. Lond. A*, **362**(1823), 2223-2238.
- Heshmati, M. and Yas, M.H. (2013), "Free vibration analysis of functionally graded CNT-reinforced nanocomposite beam using Eshelby-Mori-Tanaka approach", *J. Mech. Sci. Technol.*, **27**(11), 3403-3408.
- Hosseini-Hashemi, Rokni Damavandi Taher, S.H. and Akhavan, H. (2010), "Vibration analysis of radially FGM sectorial plates of variable thickness on elastic foundations", *Compos. Struct.*, **92**(7), 1734-1743.
- Hosseini-Hashemi, S., Es'haghi, M. and Karimi, M. (2010), "Closed-form vibration analysis of thick annular functionally graded plates with integrated piezoelectric layers", *Int. J. Mech. Sci.*, **52**(3), 410-428.
- Iijima, S. (1991), "Helical microtubes of graphitic carbon", *Nature*, **354**, 56-58.
- Kamarian, S., Yas, M.H. and Pourasghar, A. (2013), "Free vibration analysis of three-parameter functionally graded material sandwich plates resting on Pasternak foundations", *J. Sandw. Struct. Mater.*, **15**(3), 292-308.
- Kamarian, S., Shakeri, M., Yas, M.H., Bodaghi, M. and Pourasghar, A. (2015), "Free vibration analysis of functionally graded nanocomposite sandwich beams resting on Pasternak foundation by considering the agglomeration effect of CNTs", *J. Sandw. Struct. Mater.*, **17**(6), 1-31.
- Kamarian, S., Salim, M., Dimitri, R. and Tornabene, F. (2016), "Free vibration analysis of conical shells reinforced with agglomerated carbon nanotubes", *Int. J. Mech. Sci.*, **108**(1), 157-165.
- Kashalyan, M. and Menshykova, M. (2009), "Three-dimensional elasticity solution for sandwich panels with a functionally graded core", *Compos. Struct.*, **87**(1), 36-43.
- Ke, L.L., Yang, J. and Kitipornchai, S. (2010), "Nonlinear free vibration of functionally graded carbon nanotube-reinforced composite beams", *Compos. Struct.*, **92**(3), 676-683.
- Koizumi, M. (1993), "The concept of FGM, ceramic transactions", *Funct. Gradient. Mater.*, **34**, 3-10.
- Li, Q., Iu, V. and Kou, K. (2008), "Three-dimensional vibration analysis of functionally graded material sandwich plates", *J. Sound Vib.*, **311**(1-2), 498-515.
- Marin, M. (2010), "A domain of influence theorem for microstretch elastic materials", *Nonlinear Anal. Real World Appl.*, **11**(5), 3446-3452.
- Marin, M. and Lupu, M. (1998), "On harmonic vibrations in thermoelasticity of micropolar bodies", *J. Vib. Control*, **4**(5), 507-518.
- Malekzadeh, P., Golbahar Haghighi, M.R. and Atashi, M.M. (2011), "Free vibration analysis of elastically supported functionally graded annular plates subjected to thermal environment", *Meccanica*, **46**(5) 893-913.
- Matsunaga, H. (2000), "Vibration and stability of thick plates on elastic foundations", *J. Eng. Mech. ASCE*, **126**, 27-34.
- Matsunaga, H. (2008), "Free vibration and stability of functionally graded plates according to a 2D higher-order deformation theory", *J. Compos. Struct.*, **82**(4), 499-512.
- Moniruzzaman, M. and Winey, K.I. (2006), "Polymer nanocomposites containing carbon nanotubes", *Macromolecules*, **39**(16), 5194-5205.
- Moradi-Dastjerdi, R., Pourasghar, A. and Foroutan, M. (2013), "The effects of carbon nanotube orientation and aggregation on vibrational behavior of functionally graded nanocomposite cylinders by a mesh-free method", *Acta Mech.*, **224**(11), 2817-2832.
- Nie, G.J. and Zhong, Z. (2008), "Vibration analysis of functionally graded annular sectorial plates with simply supported radial edges", *Compos. Struct.*, **84**(2), 167-176.
- Odegard, G.M., Gates, T.S., Wise, K.E., Park, C. and Siochi, E.J. (2003), "Constitutive modelling of nanotube reinforced polymer composites", *Compos. Sci. Technol.*, **63**(11), 1671-1687.
- Qian, D., Dickey, E.C., Andrews, R. and Rantell, T. (2000), "Load transfer and deformation mechanisms in carbon nanotube-polystyrene composites", *Appl. Phys. Lett.*, **76**(20), 2868-2870.
- Salvetat, D. and Rubio, A. (2002), "Mechanical properties of carbon nanotubes: a fiber digest for beginners", *Carbon*, **40**(10), 1729-1734.
- Seidel, G.D. and Lagoudas, D.C. (2006), "Micromechanical

- analysis of the effective elastic properties of carbon nanotube reinforced composites”, *Mech. Mater.*, **38**(8-10) 884-907.
- Shaffer, M.S.P. and Windle, A.H. (1999), “Fabrication and Characterization of Carbon Nanotube/Poly (vinyl alcohol) Composites”, *Adv. Mater. (Weinheim, Ger.)*, **11**(11), 937-941.
- Sharma, K. and Marin, M. (2013), “Effect of distinct conductive and thermodynamic temperatures on the reflection of plane waves in micropolar elastic half-space”, *U.P.B. Sci. Bull., Series A-Appl. Math. Phys.*, **75**(2), 121-132.
- Shen, H.S. (2009), “Nonlinear bending of functionally graded carbon nanotube-reinforced composite plates in thermal environments”, *Compos. Struct.*, **91**(1), 9-19.
- Shen, H.S. and Zhang, C.L. (2010), “Thermal buckling and postbuckling behavior of functionally graded carbon nanotube-reinforced composite plates”, *Mater. Des.*, **31**(7), 3403-3411.
- Shen, H.S. and Zhu, Z.H. (2010), “Buckling and postbuckling behavior of functionally graded nanotube-reinforced composite plates in thermal environments”, *Comput. Mater Continua.*, **18**(2), 155-182.
- Shi, D.L., Feng, X.Q., Huang, Y.Y., Hwang, K.C. and Gao, H. (2004), “The effect of nanotube waviness and agglomeration on the elastic property of carbon nanotube reinforced composites”, *J. Eng. Mater. Technol.*, **126**(3) 250-257.
- Shokrieh, M.M. and Rafiee, R. (2010a), “Investigation of nanotube length effect on the reinforcement efficiency in carbon nanotube based composites”, *Compos. Struct.*, **92**(10), 2415-2420.
- Shokrieh, M.M. and Rafiee, R. (2010b), “Prediction of mechanical properties of an embedded carbon nanotube in polymer matrix based on developing an equivalent long fiber”, *Mech. Res. Commun.*, **37**(2), 235-240.
- Shu, C. (2000), *Differential Quadrature and its Application in Engineering*, Springer Science & Business Media.
- Shu, C. and Richards, B.E. (1992), “Application of generalized differential quadrature to solve two dimensional incompressible Navier-Stokes equations”, *Int. J. Numer. Methods Fluid*, **15**(7), 791-798.
- Stephan, C., Nguyen, T.P., Chappelle, M.L. and Lefrant, S. (2000), “Characterization of single-walled carbon nanotubes-PMMA composite”, *Synth. Met.*, **108**(2), 139-149.
- Tahouneh, V. (2014a), “Free vibration analysis of bidirectional functionally graded annular plates resting on elastic foundations using differential quadrature method”, *Struct. Eng. Mech., Int. J.*, **52**(4), 663-686.
- Tahouneh, V. (2014b), “Free vibration analysis of thick CGFR annular sector plates resting on elastic foundations”, *Struct. Eng. Mech., Int. J.*, **50**(6), 773-796.
- Tahouneh, V. (2016), “Using an equivalent continuum model for 3D dynamic analysis of nanocomposite plates”, *Steel Compos. Struct., Int. J.*, **20**(3), 623-649.
- Tahouneh, V. and Naei, M.H. (2014), “A novel 2-D six-parameter power-law distribution for three-dimensional dynamic analysis of thick multi-directional functionally graded rectangular plates resting on a two-parameter elastic foundation”, *Meccanica*, **49**(1), 91-109.
- Tahouneh, V. and Naei, M.H. (2016), “Free vibration and vibrational displacements analysis of thick elastically supported laminated curved panels with power-law distribution functionally graded layers and finite length via 2D GDQ method”, *J. Sandw. Struct. Mater.*, **18**(3), 263-293.
- Tahouneh, V. and Yas, M.H. (2012), “3-D free vibration analysis of thick functionally graded annular sector plates on Pasternak elastic foundation via 2-D differential quadrature method”, *Acta Mech.*, **223**(9), 1879-1897.
- Tahouneh, V. and Yas, M.H. (2013), “Semi-analytical solution for three-dimensional vibration analysis of thick multidirectional functionally graded annular sector plates under various boundary conditions”, *J. Eng. Mech.*, **140**(1), 31-46.
- Tahouneh, V., Yas, M.H., Tourang, H. and Kabirian, M. (2013), “Semi-analytical solution for three-dimensional vibration of thick continuous grading fiber reinforced (CGFR) annular plates on Pasternak elastic foundations with arbitrary boundary conditions on their circular edges”, *Meccanica*, **48**(6), 1313-1336.
- Thostenson, E.T., Ren, Z.F. and Chou, T.W. (2001), “Advances in the Science and Technology of Carbon Nanotubes and their Composites: A Review”, *Compos. Sci. Technol.*, **61**(13), 1899-1912.
- Tornabene, F. and Viola, E. (2009), “Free vibration analysis of four-parameter functionally graded parabolic panels and shells of revolution”, *Eur. J. Mech. A/Solid*, **28**(5), 991-1013.
- Tornabene, F., Fantuzzi, N. and Ubertini, F. (2015), “Strong formulation finite element method based on differential quadrature: A survey”, *Appl. Mech. Rev.*, **67**(2), 1-55.
- Tornabene, F., Fantuzzi, N., Bacciocchi, M. and Viola, E. (2016), “Effect of agglomeration on the natural frequencies of functionally graded carbon nanotube-reinforced laminated composite doubly-curved shells”, *Compos. Part B*, **89**(1), 187-218.
- Tsai, S.W., Hoa, C.V. and Gay, D. (2003), *Composite Materials, Design and Applications*, CRC Press, Boca Raton, CA, USA.
- Valter, B., Ram, M.K. and Nicolini, C. (2002), “Synthesis of multiwalled carbon nanotubes and poly (o-anisidine) nanocomposite material: Fabrication and characterization its langmuir-schaefer films”, *Langmuir*, **18**(5), 1535-1541.
- Vigolo, B., Penicaud, A.P., Couloun, C., Sauder, S., Paillet, R., Journet, C., Bernier, P. and Poulin, P. (2000), “Macroscopic fibers and ribbons of oriented carbon nanotubes”, *Science*, **290**(5495), 1331-1334.
- Wagner, H.D., Lourie, O. and Feldman, Y. (1997), “Stress-induced fragmentation of multiwall carbon nanotubes in a polymer matrix”, *Appl. Phys. Lett.*, **72**(2), 188-190.
- Wang, Z.X. and Shen, H.S. (2011), “Nonlinear vibration and bending of sandwich plates with nanotube-reinforced composite face sheets”, *Compos. Part B*, **43**(2), 411-421.
- Wernik, J.M. and Meguid, S.A. (2011), “Multiscale modeling of the nonlinear response of nano-reinforced polymers”, *Acta Mech.*, **217**(1), 1-16.
- Wuite, J. and Adali, S. (2005), “Deflection and stress behaviour of nanocomposite reinforced beams using a multiscale analysis”, *Compos. Struct.*, **71**(3-4), 388-396.
- Yas, M.H. and Sobhani Aragh, B. (2010), “Free vibration analysis of continuous grading fiber reinforced plates on elastic foundation”, *Int. J. Eng. Sci.*, **48**(12), 1881-1895.
- Yas, M.H. and Tahouneh, V. (2012), “3-D free vibration analysis of thick functionally graded annular plates on Pasternak elastic foundation via differential quadrature method (DQM)”, *Acta Mech.*, **223**(1), 43-62.
- Yokozeki, T., Iwahori, Y. and Ishiwata, S. (2007), “Matrix cracking behaviors in carbon fiber/epoxy laminates filled with cup-stacked carbon nanotubes (CSCNTs)”, *Compos. Part A*, **38**(3), 917-924.
- Zenkour, A. (2005a), “A comprehensive analysis of functionally graded sandwich plates, Part 1-Deflection and stresses”, *Int. J. Solids Struct.*, **42**(18-19), 5224-5242.
- Zenkour, A. (2005b), “A comprehensive analysis of functionally graded sandwich plates: Part 2-Buckling and free vibration”, *Int. J. Solids Struct.*, **42**(18-19), 5243-5258.
- Zhou, D., Cheung, Y.K., Lo, S.H. and Au, F.T.K. (2004), “Three-dimensional vibration analysis of rectangular thick plates on Pasternak foundation”, *Int. J. Numer. Methods Eng.*, **59**(10), 1313-1334.